Computer Simulations of Domain Pattern Formation in Ferroelectrics

Rajeev Ahluwalia and Wenwu Cao

Materials Research Lab, The Pennsylvania State University, PA 16802,USA

Abstract. We study domain pattern formation in ferroelectrics based on a 2-D time-dependent Ginzburg Landau theory. The model includes electrostrictive and elastic effects in the form of a long-range interaction between the polarization fields that is obtained by eliminating the strain fields subject to the elastic compatibility constraint. We simulate a 2-D square to rectangle transition that has four equivalent polarization states in the ferroelectric phase. Starting from an unstable paraelectric state, we simulate the domain pattern evolution in the absence of external electric field. For the case without defects, the final pattern is a twinned state that has only head to tail (uncharged) domain walls. However, for the case with randomly distributed dipolar defects, head to head and tail to tail charged walls are observed. These results are in accordance with recent experiments where charged domain walls have been observed.

It is now well established that the ferroelectric transformation is accompanied by the formation of domains of the low temperature phase states. Ferroelectric materials that have only two polarization states usually form strain free 180° domains. However for multiple degenerate systems, such as $BaTiO_3$ and PZT, the electrostrictively generated strain is responsible for the creation of 90° domain walls. It is important to understand the mechanism of formation of these domain structures as physical properties like the dielectric constant and hysteresis are mainly governed by motion of the domain walls.

A useful technique to study the domain pattern formation in phase transitions is the time-dependent Ginzburg Landau (TDGL) theory. In the context of ferroelectric phase transitions, this approach has been sucessfully used to study the formation and growth of domains [1-4]. In this article, we use a TDGL model to study pattern formation in a model 2-D ferroelectric system that has four degenerate polarization states. We also include the electrostrictive coupling of polarization with the strain and the contributions due to randomly distributed dipolar defects.

The 3-D free-energy including strain and electrostrictive coupling has been given before [5]. For simplicity, we consider a 2-D square to rectangle ferroelectric transition in the absence of an external field with free-energy given as

CP582, *Fundamental Physics of Ferroelectrics 2001*, edited by H. Krakauer

$$F = \int d\vec{r}[f_l + f_g + f_{el} + f_{es} + f_d] \tag{1}$$

where f_l is a Landau free energy density given as

$$f_l = \frac{\alpha_1}{2}(P_x^2 + P_y^2) + \frac{\alpha_{11}}{4}(P_x^4 + P_y^4) + \frac{\alpha_{12}}{2}P_x^2 P_y^2 \tag{2}$$

Here, f_l is identical to the free energy density used in earlier works [4,5]. The gradient energy f_g is given as

$$f_g = \frac{g_1}{2}[(\frac{\partial P_x}{\partial x})^2 + (\frac{\partial P_y}{\partial y})^2] + \frac{g_2}{2}[(\frac{\partial P_x}{\partial y})^2 + (\frac{\partial P_y}{\partial x})^2] + g_3(\frac{\partial P_x}{\partial x})(\frac{\partial P_y}{\partial y}). \tag{3}$$

The free energy contribution due to randomly distributed dipolar defects is given as $f_d = -\vec{E}_d \cdot \vec{P}$, where $\vec{E}_d(\vec{r}) = -\vec{\nabla}V_d(\vec{r})$. The potential V_d represents a configuration of randomly placed defect dipoles given as

$$V_d(\vec{r}_i) = \sum_j^{n_d}[\frac{1}{|\vec{r}_i - (\vec{r}_j + \vec{\delta})|} - \frac{1}{|\vec{r}_i - (\vec{r}_j - \vec{\delta})|}]q_0(\vec{r}_j) \tag{4}$$

Here q_0 represents the coarse-grained charge and δ the displacement associated with the defect dipole centered at $\vec{r}_j$. The elastic energy of the system can be written in terms of the bulk strain $\phi_1 = (\eta_{xx} + \eta_{yy})/\sqrt{2}$, the deviatoric strain $\phi_2 = (\eta_{xx} - \eta_{yy})/\sqrt{2}$ and the shear strain $\phi_3 = \eta_{xy} = \eta_{yx}$. Here η_{ij} is the linear elastic strain tensor. The elastic free energy can then be written as

$$f_{el} = \frac{a_1}{2}\phi_1^2 + \frac{a_2}{2}\phi_2^2 + \frac{a_3}{2}\phi_3^2 \tag{5}$$

where a_1, a_2 and a_3 are linear combinations of second order elastic constants. Similarly, the electrostrictive energy in terms of the electrostrictive constants q_1, q_2 and q_3 is given as

$$f_{es} = -q_1\phi_1(P_x^2 + P_y^2) - q_2\phi_2(P_x^2 - P_y^2) - q_3\phi_3 P_x P_y \tag{6}$$

Following the methodology used in earlier work [4], the elastic and electrostrictive contributions can be expressed as an effective long-range interaction between the polarization fields by eliminating the strain fields subject to the elastic compatibility conditions. The effective long-range interaction in fourier space is then given as

$$F_{eff} = \frac{q_2^2}{2a_2}\int d\vec{k} H(\vec{k}) \left|\Gamma_2(\vec{k})\right|^2 \tag{7}$$

$$\mathrm{H}(\vec{\mathrm{k}}) = \mathrm{h}_1^2(\vec{\mathrm{k}})/\alpha + \mathrm{h}_2^2(\vec{\mathrm{k}}) - 2\mathrm{h}_2(\vec{\mathrm{k}}) + \mathrm{h}_3^2(\vec{\mathrm{k}})/\beta \tag{8}$$

and $\Gamma_2(\vec{k})$ is the fourier transform of $P_x^2 - P_y^2$. The quantities $\mathrm{h}_1, \mathrm{h}_2$ and h_3 are given as $h_1(\vec{k}) = k^2 Q(\vec{k})$, $h_2(\vec{k}) = [1 - (k_x^2 - k_y^2)Q(\vec{k})]$ and $h_3(\vec{k}) = -\sqrt{8}k_x k_y Q(\vec{k})$, where

$$\mathrm{Q}(\vec{\mathrm{k}}) = \frac{(\mathrm{k}_x^2 - \mathrm{k}_y^2)}{(\mathrm{k}^4/\alpha + (\mathrm{k}_x^2 - \mathrm{k}_y^2)^2 + 8\mathrm{k}_x^2\mathrm{k}_y^2/\beta)} \tag{9}$$

where $\alpha = a_1/a_2$ and $\beta = a_3/a_2$. Here, we should remark that the above interaction has been obtained by assuming no coupling of the polarization with bulk and shear strains, i.e., $q_1 \to 0$ and $q_3 \to 0$. In order to catch the essential physics and reduce the computational difficulties, the coupling to bulk and shear strains are not included in this work. Based on experimental results, the bulk strain is small in most of the ferroelectric materials and the shear strain does not exist at all the single domain regions for the case under study. Thus we believe that this assumption will not introduce significant errors in the study of domain pattern formation.

In order to study the dynamics of domain pattern formation, we make use of the time-dependent Ginzburg-Landau equations (TDGL). We introduce rescaled variables as follows: $\mathrm{t} = (\mathrm{t}^*/|\alpha_1|\mathrm{L})$, where L is the kinetic coefficient, $\vec{\mathrm{r}}^* = \vec{\mathrm{r}}/\phi$ $(\phi = \sqrt{g_1/a|\alpha_1|})$, where a is a dimensionless constant. The polarization is transformed as $P_x = P_R u$ and $P_y = P_R v$, where $\mathrm{P_R} = \sqrt{|\alpha_1|/\alpha_{11}}$ is the remnant polarization of the homogeneous state without elastic effects. With this set of rescaled parameters, the TDGL equations are given as

$$\begin{aligned}
\mathrm{u}_{,t^*} &= \mathrm{u} - \mathrm{u}^3 - \mathrm{duv}^2 + \mathrm{au}_{,x^*x^*} + \mathrm{bu}_{,y^*y^*} + \mathrm{cv}_{,x^*y^*} + \varepsilon_x \\
&\quad - \gamma \mathrm{u}\int d\vec{\mathrm{k}}^* \mathrm{H}(\vec{\mathrm{k}}^*)\Gamma(\vec{\mathrm{k}}^*)\exp(-i\vec{\mathrm{k}}^* \bullet \mathrm{r}^*) \\
\mathrm{v}_{,t^*} &= \mathrm{v} - \mathrm{v}^3 - \mathrm{dvu}^2 + \mathrm{av}_{,x^*x^*} + \mathrm{bv}_{,y^*y^*} + \mathrm{cu}_{,x^*y^*} + \varepsilon_y \\
&\quad + \gamma \mathrm{v}\int d\vec{\mathrm{k}}^* \mathrm{H}(\vec{\mathrm{k}}^*)\Gamma(\vec{\mathrm{k}}^*)\exp(-i\vec{\mathrm{k}}^* \bullet \mathrm{r}^*)
\end{aligned} \tag{10}$$

Here $\vec{\varepsilon}$ is the rescaled electric field due to the randomly distributed defect dipoles, with $q_0^*(\vec{r}^*) = [q_0(\vec{r})/P_R\phi^2|\alpha_1|]$. In the rescaled equations, the constant

$d=(\alpha_{12}/\alpha_{11})$, $\gamma=(q_2{}^2/\alpha_{11}a_2)$, $b=(g_2/|\alpha_1|\phi^2)$ and $c=(g_3/|\alpha_1|\phi^2)$. $\Gamma(\vec{k}^*)$ is the fourier transform of u^2-v^2.

To study the domain patterns, equation (10) is discretized using finite differences on a 128×128 grid with periodic boundary conditions. The space discretization step is set as $\Delta x^* = \Delta y^* = 1$ and the time interval $\Delta t^* = 0.02$. The parameters chosen for the simulation are $d=2$ and $\gamma=0.05$. The gradient coefficients are chosen as $a=b=c=10$ and the elastic parameters are $\alpha=\beta=1$. We first describe the simulation of domain pattern formation for the case without dipolar defects ($\varepsilon_x = \varepsilon_y = 0$), starting from small amplitude initial conditions corresponding to a paraelectric phase. Figure 1 displays the time evolution of domains for the defect free case. The direction of the arrows in figure 1 is the polarization direction and the magnitude is proportional to the length. In figure 1(a) ($t^* = 0.5$) we can clearly see the appearance of domains with non-zero polarization. However, these domains are still randomly oriented. In figure 1(b) ($t^*=12.5$), four distinct kind of polarization domains corresponding to the minnima of equation (2) can be observed. Note that at this stage both charged as well as uncharged domain walls are observed. We can also observe that the domain walls are beginning to get oriented along [11]or $[1\bar{1}]$. This is due to the long-range anisotropic interaction which prefers alignment along the 45° directions. As we go further in time, the domain walls move in order to get rid of the head to head and tail to tail configurations. As we can observe in figure 1(c)($t^*=125$), head to tail domain walls aligned along [11]or $[1\bar{1}]$ are dominant. Finally, in figure 1(d) ($t^*=500$), we can see that we have a twinned pattern that has only head to tail uncharged domain walls.

Next, we describe our results for pattern evolution for the case with defects. For the defect field $\vec{\varepsilon}$, we take $q_0{}^*$ to be uniformly distributed in the interval [0.01,0.03]. The charge separation $\vec{\delta}^*$ can take the value $(\pm c,0)$ or $(0,\pm c)$, where c is a random number uniformly distributed in the interval [0.08,0.1]. The defect field is initialized by selecting random points on the discrete grid. We choose the number of defects to $n_d = 327$ (2% of the total number of grid points). The initial conditions for the polarization fields are the same as in the defect free case. In figure 2(a)($t^* = 0.5$), we can see the early time snapshot where most of the system is still paraelectric. It is clear that randomly distributed dipoles locally try to align the polarization. These defects strongly influence the dynamics and the eventual state. In figure 2(b)($t^* = 25$), we can see domains of all four degenerate states coexisting. Interestingly, the number of charged and 180° walls for this case is much more compared to the defect free case at similar stages of the evolution. We believe that this is due to the dipolar defects which locally influence the domain pattern and lead to a pinning of the domains, which makes the domain dynamics slower. The system tries to get rid of charged walls, as can be seen by comparing figure 2(b) and figure 2(c)($t^* = 250$). However, in this case the system gets arrested in a metastable state

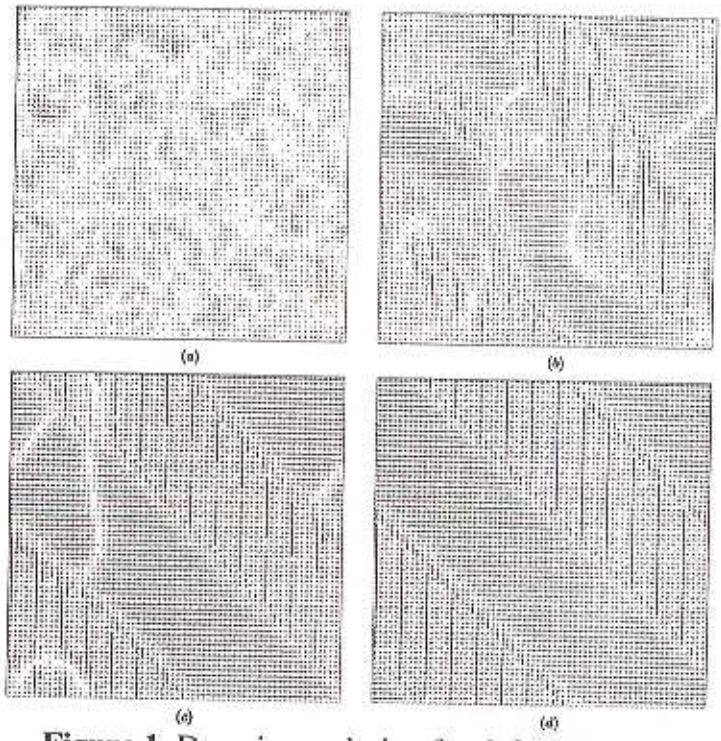

Figure 1. Domain evolution for defect free case

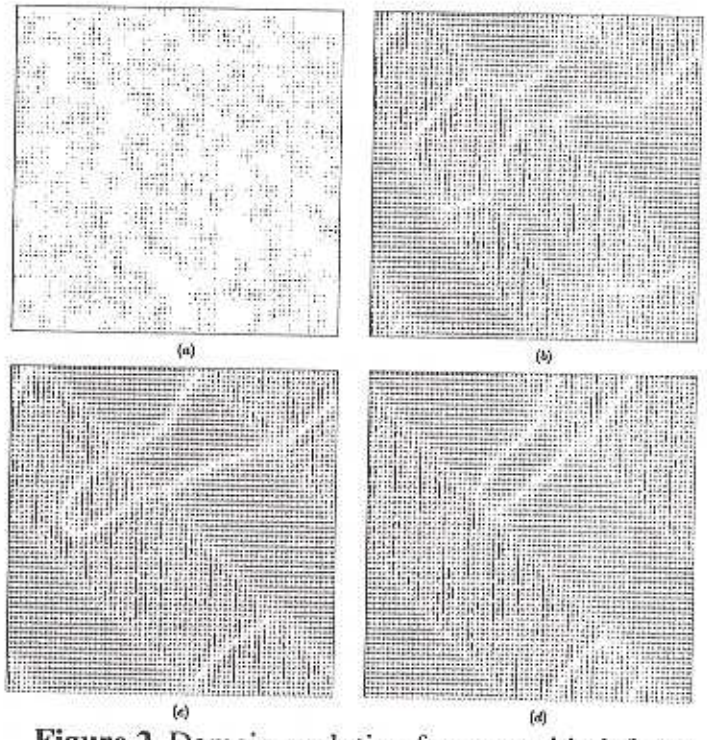

Figure 2. Domain evolution for case with defects

that has charged as well as uncharged walls. This is clear from figure 2(d) ($t^* = 1000$), which is the final state as running the simulation longer does not change the domain pattern noticeably.

To conclude, we have made a study of domain pattern formation in ferroelectrics based on the TDGL approach and incorporating elastic coupling. Domain structures evolve with time with domain walls oriented along the [11] or [1 $\bar{1}$] directions. This wall direction is preferred to ensure the strain compatibility at the interfaces. For the case with defects, we find that in addition to the uncharged 90° walls, charged walls and 180° walls are stabilized due to the dipolar defects. These results are agreement with recent experiments on PZN-PT single crystals [6]. Although, our model is phenomenological, we have been able to simulate the ferroelectric microstructure qualitatively based on a coarse grained picture. Unfortunately, not all coefficients in the Landau theories are experimentally measured which makes it difficult to give more quantitative predictions. However, our results have demonstrated that the TDGL theory can be used to simulate domain related phenomena in ferroelectric systems if all parameters are measured experimentally.

ACKNOWLEDGEMENT

We acknowledge the support of Office of Naval Research.

REFERENCES

1. S. Nambu and D.A. Sagala, Phys. Rev. B 50, 5838(1994)
2. H.L Hu and L.Q. Chen, Materials. Science. Engineering A 238, 182(1997)
3. W. Cao, S. Tavener and S. Xie, J. Appl. Phys. 86, 5793(1999)
4. R. Ahluwalia and W. Cao, Phys. Rev. B 63, 012103(2001)
5. W. Cao and L. E. Cross, Phys. Rev. B 44, 5(1991)
6. J. Yin and W. Cao, J. Appl. Phys. 87, 133(2000)